HNPS Advances in Nuclear Physics

Vol 3 (1992)

HNPS1992

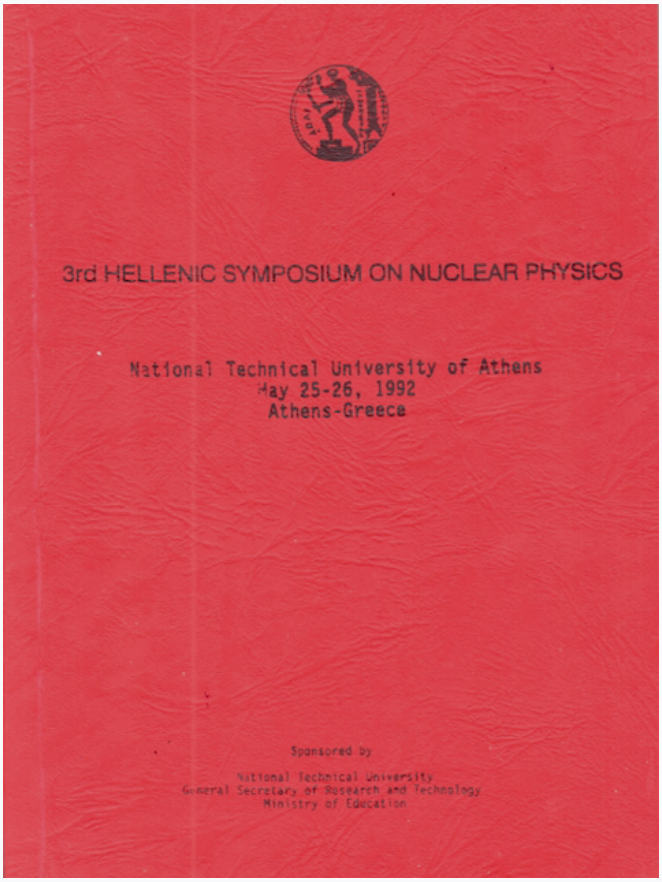

Determination of Dipole Polarization Effects in 7Li and 11Li

L. D. Skouras, H. Muther, M. A. Nagarajan

doi: 10.12681/hnps.2381

Determination of Dipole Polarization Effects in ^{7}Li and ^{11}Li†

L.D. Skouras[1], H. Müther[2] and M.A. Nagarajan[3]
[1] Institute of Nuclear Physics, NRCPS *Demokritos*, GR-15310 Aghia Paraskevi Attiki, Greece
[2] Institut für Theoretische Physik der Universität Tübingen, D-7400 Tübingen Federal Republic of Germany
[3] SERC Daresbury Laboratory, Daresbury, Warrington WA4 4AD, UK

Abstract: The structure of ^{6}Li, ^{7}Li and ^{11}Li nuclei is investigated in a model space which includes all configurations with oscillator energy up to $3\hbar\omega$ above the ground state configuration. The energy spectra and electromagnetic properties of the low-lying states are determined with various two-body interactions, which are derived from the Bonn potential. In addition the calculation determines the *dipole polarizability* of ^{7}Li and ^{11}Li caused from virtual $E1$ excitations to the positive parity states of these nuclei.

1. Introduction

The static and dynamic electric moments of nuclei are traditionally measured by Coulomb excitation[1]). It has long been established that the quadrupole moments as well as the $B(E2)$ values can be affected from virtual excitations to the giant dipole state[2]). In particular, if the dipole state occurs at low excitation energy, it can cause a measurable renormalization of the $E2$ operator.

The most careful measurements of the correction due to the dynamic *dipole polarizability* on the $B(E2)$ and the quadrupole moments has been in the case of the nucleus ^{7}Li [3-4]). This nucleus has a ground state with $J^{\pi} = 3/2^{-}$ and a first excited state with $J^{\pi} = 1/2^{-}$. The excited state has no spectroscopic quadrupole moment and hence a precise determination of the $B(E2)\uparrow$ value for the excitation of the $1/2^{-}$ state over a range of energies will enable one to measure the *inelastic dipole polarizability*. Similarly, a careful measurement of the ground state quadrupole moment will enable one to measure the *elastic dipole polarizability*. The results of various measurements are reviewed by Barker *et al* [5]) and Voelk and Fick[6]).

Recent experiments[7]) suggest that a component of the dipole resonance, termed *the soft dipole mode*[8]) or *the pygmy resonance*[9]), occurs at a very low excitation in ^{11}Li. This feature combined with the large r_{ms} radius of $3.16 \pm 0.11 fm$ [10]) have made this nucleus the subject of several theoretical investigations.

† Presented by L.D. Skouras

In this paper we present a shell-model study of the natural parity states of ^{6}Li, ^{7}Li and ^{11}Li. The properties of these states are investigated in the space of $(0+2)\hbar\omega$ excitations. For ^{7}Li and ^{11}Li we also examine the unnatural parity states for which we consider the complete space of $(1+3)\hbar\omega$ excitations. The most detailed data exist for ^{7}Li and we use them to draw conclusions about the reliability of our model. On the other hand, there exist very little data for ^{11}Li and thus our results should be taken as theoretical predictions.

The main purpose of our investigation has been to determine the $E1$ polarization effects on the quadrupole moment of the $3/2^-$ ground state of both ^{7}Li and ^{11}Li as well as on the $B(E2)\uparrow$ value corresponding to the excitation of the $1/2^-$ state of ^{7}Li. Several sets of results have been determined corresponding to different hamiltonians. To test the reliability of these calculations we have also determined the properties of the low-lying states of ^{6}Li, ^{7}Li and ^{11}Li and compare the theoretical predictions with the existing experimental data.

In sect. 2 we discuss the details of our calculation, while in sect. 3 we present our results. Finally, sect. 4 contains the conclusions of this work.

2. Details of the calculation

2.1 Definitions

The effective potential which is used to describe $E2$ excitation of the projectile in Coulomb scattering experiments consists of two parts[1]) :

$$V_{E2} = V_{coup} + V_{pol} \quad , \tag{1}$$

where

$$\langle f|V_{coup}(\vec{r})|i\rangle = \frac{4\pi}{5}\frac{Ze}{r^3}\langle J_f||E2||J_i\rangle X^{J_f J_i}_{M_f M_i}(\hat{r}) \quad , \tag{2}$$

$$\langle f|V_{pol}(\vec{r})|i\rangle = -\frac{Z^2e^2}{r^4}[\delta_{if}P + \sqrt{\frac{9\pi}{5}}(-1)^{J_f-J_i}\tau_{if}X^{J_f J_i}_{M_f M_i}(\hat{r})] \quad , \tag{3}$$

with

$$X^{J_f J_i}_{M_f M_i}(\hat{r}) = \frac{1}{(2J_f+1)^{1/2}}\sum_{\mu} Y^*_{2\mu}(\hat{r})\langle J_i M_i 2\mu|J_f M_f\rangle \tag{4}$$

In the above eqs (2)-(4), Z is the charge number of the target, $\vec{r}$ is the distance between the two nuclei, while $|f\rangle$ and $|i\rangle$ denote the final and initial states of the projectile, respectively.

The polarization potential (3) consists of a monopole and a quadrupole term. The monopole term is defined[1]) as:

$$P = \frac{4\pi}{9} \sum_n \frac{B(E1; i \to n)}{(E_n - E_i)} \tag{5}$$

where

$$B(E\lambda; i \to f) = \frac{\langle f||E\lambda||i\rangle^2}{2J_i + 1} \tag{6}$$

and $|n\rangle$ are the states which are connected by the $E1$ operator with the state $|i\rangle$.

The quantity τ_{if} in the quadrupole part of V_{pol} is the tensor moment of the electric polarizability and is defined[3]) as:

$$\tau_{if} = \frac{8\pi}{9}\sqrt{\frac{10}{3}} \sum_n W(11J_fJ_i; 2J_n) \frac{\langle i||E1||n\rangle\langle n||E1||f\rangle}{(E_n - E_i)} \tag{7}$$

From the analyses of the ^{7}Li data[5,6]) values for four quantities have been extracted. These are $B(E2; 1 \to 2)$, τ_{12}, τ_{11} and the static quadrupole moment Q_s. We use here the notation usually adopted[5,6]) where 1 refers to the ground state and 2 to the first excited state. Q_s is defined as:

$$Q_s = \sqrt{\frac{16\pi}{5}} \sqrt{\frac{J_i(2J_i - 1)}{(J_i + 1)(2J_i + 1)(2J_i + 3)}} \langle i||E2||i\rangle \quad . \tag{8}$$

The experimental values for these four quantities are compared with the predictions of the calculation in sect. 3.

2.2 The shell-model calculation

We consider a hamiltonian of the form

$$H = \sum_i^A t_i + \sum_{i<j}^A G_{ij} + \frac{1}{2} Am\omega^2 R^2 - \frac{3}{2}\hbar\omega \quad , \tag{9}$$

where t denotes kinetic energy, G is the two-body interaction while A and $\vec{R}$ stand for the mass number and center-of-mass coordinate of the nucleus, respectively. The term $\frac{1}{2}Am\omega^2R^2$ has been included in the hamiltonian H in order to remove spurious state effects[11]) while the term $-\frac{3}{2}\hbar\omega$ removes the center-of-mass contribution from a non-spurious state. The hamiltonian (9) can be written as:

$$H = H_0 + V \quad , \tag{10}$$

where

$$H_0 = \sum_i^A (t_i + \frac{1}{2}m\omega^2 r_i^2) - \frac{3}{2}\hbar\omega \; , \qquad V = \sum_{i<j}^A (G_{ij} - \frac{m\omega^2}{2A}(\vec{r}_i - \vec{r}_j)^2) \quad . \tag{11}$$

The basis of our calculation consists of all eigenvectors of H_0 which have unperturbed energy not exceeding by $3\hbar\omega$ the energy of the ground state configuration $(0s)^4(0p)^{A-4}$. Thus the model space contains 15 single particle orbitals from the $0s$ up to the *sdg* shell of the harmonic oscillator potential. The basis vectors are constructed assuming no core state and are represented as

$$|\Phi\rangle = |C^A; JT\mu\rangle \quad , \tag{12}$$

where C^A denotes a distribution of the A particles among the single particle-orbitals, while the index μ distinguishes the vectors which correspond to the same set of $\{C^A, J, T\}$ quantum numbers.

Since the vectors (12) have been constructed using isospin formalism it is convenient to consider in the same formalism the operators $E\lambda$ of sect. 2.1. Thus

$$E^\lambda_\mu = E^{\lambda 0}_{\mu 0} + E^{\lambda 1}_{\mu 0} \quad , \tag{13}$$

where

$$E^{\lambda 0}_{\mu 0} = \frac{e}{2}\sum_i^A r_i^\lambda Y_{\lambda\mu}(\hat{r}_i) \; , \quad E^{\lambda 1}_{\mu 0} = \frac{e}{2}\sum_i^A \tau_0(i) r_i^\lambda Y_{\lambda\mu}(\hat{r}_i) \quad . \tag{14}$$

Thus the matrix elements of the operator $E\lambda$ can be expressed as:

$$\langle J_f T_f M_T || E^\lambda || J_i T_i M_T\rangle =$$

$$\frac{\delta_{T_f T_i}\langle J_f T_f || E^{\lambda 0} || J_i T_i\rangle + \langle J_f T_f || E^{\lambda 1} || J_i T_i\rangle \langle T_i M_T 10 | T_f M_T\rangle}{(2T_f+1)^{1/2}} \tag{15}$$

where

$$M_T = \frac{Z-N}{2} \quad , \tag{16}$$

Z and N being the proton and neutron numbers of the nucleus under consideration. In (15) and elsewhere a triple bar denotes a matrix element which is reduced in both spin and isospin spaces.

As is evident from (14), the isoscalar part of the $E1$ operator is proportional to the center-of-mass vector $\vec{R}$. Thus the E^{10} operator connects a non-spurious natural parity state to a spurious one, which belongs to the space of the unnatural parity states. As a consequence only the isovector part of the $E1$ operator is considered in determining $E1$ matrix elements (15).

As eqs (5) and (7) indicate, to obtain the matrix elements of V_{pol} one needs to determine all states $|n\rangle$ which are connected to both $|i\rangle$ and $|f\rangle$ by the $E1$ operator. The main problem with the determination of these intermediate states $|n\rangle$ is that their space consists of the $(1+3)\hbar\omega$ excitations and, consequently, it has a large dimension (over 3000 for some states of ^{11}Li). In addition the relatively few of the states $|n\rangle$ which are strongly connected by the $E1$ operator to the $|i\rangle$ and $|f\rangle$ states need not necessarily be among the lowest in energy. Thus, in principle, one needs to perform a full diagonalization of the hamiltonian matrix in the space of $(1+3)\hbar\omega$ excitations. Apart from the technical difficulties, this solution has the disadvantage that most of the eigenstates $|n\rangle$ produced will couple only weakly to the initial and final states. To face the above problem, we have adopted the BAGEL approach of Skouras and Müther[12]) which is suitable for selecting specific eigenstates of a hamiltonian matrix of large dimension.

2.3 Two-body interaction and oscillator parameter

In this section we discuss the determination of the two-body interaction G that appears in eq. (9) and also the manner in which we selected the value of the oscillator parameter $b = (\hbar/m\omega)^{1/2}$ which is used to define the basis of single-particle states as presented in (11).

The matrix elements of G have been determined by solving the Bethe-Goldstone equation

$$G = \mathcal{V} + \mathcal{V}\frac{Q}{E_s - QtQ}G \tag{17}$$

directly in the basis of harmonic oscillator states[13]). For the starting energy E_s a constant value of -30 MeV has been adopted while the Pauli operator Q was defined to exclude any intermediate two-particle configuration which is taken into account in our shell-model calculation.

For the bare NN interaction V in (17) we have considered two versions of the Bonn OBE potential[14]). The parameters of these potentials have been adjusted to fit the NN scattering phase shifts by solving the Thompson equation. The two potentials are denoted as A and C in table A.2 of [14]) and they mainly differ in the strength of the tensor component. In the following we shall denote the G-matrices corresponding to potentials A and C by G^A and G^C, respectively.

The above potentials A and C have been used in Dirac-Brueckner-Hartree-Fock calculations for light nuclei[15]). Such calculations have shown that the Dirac spinors for nucleons in nuclear medium are substantially different from those of free nucleons. The ratio of large to small components for the Dirac spinors in the medium may be described in terms of an effective mass m^*. It has been shown[15]) that the value of $m^* = 630 MeV$ is a reasonable choice for light nuclei. In our calculation we use this value of m^* as well as the value $m^* = 938 MeV$ of the free nucleon (which means that a change of the Dirac spinors in the medium is ignored) and we shall distinguish the corresponding G-matrices by G_m and G, respectively.

The other parameter that enters our calculation is the oscillator parameter b. This is treated as a variational parameter and we adopt the value of b for which the binding energy of each nucleus is a minimum. This procedure has been repeated for each G-matrix considered in the calculation.

3. Results of the calculation

As outlined in sect. 2.3, in our calculation we have considered four types of two-body matrix elements. These correspond to using as V in eq. (17) versions A and C of the Bonn potential[14]) and values of 938 MeV and 630 MeV for the parameter m^*. In the following we shall distinguish the results corresponding to these four sets by G^A, G^C, G^A_m and G^C_m.

All the G-matrices described above were determined for the values of 1.6, 1.8, 2.0 and 2.1 fm for the oscillator parameter b. Thus, altogether, 16 sets of two-body matrix elements were determined and the properties of the low- lying states of ^{6}Li and ^{7}Li were calculated for all these interactions. Since a calculation of ^{11}Li in the large model space under consideration requires a large amount of computer time a more restrictive selection has been made for this isotope.

Table 1 shows the dependence of the binding energy on the interaction and the oscillator parameter. The experimental values for this quantity are[16]) -31.99, -39.25 and -45.54 MeV for ^{6}Li, ^{7}Li and ^{11}Li, respectively. As seen in this table, all interactions considered in the calculation greatly underestimate the binding energies of the Li isotopes. The differences obtained for the various interactions can be understood as follows: (i) The OBE potential with a weaker tensor component (A) yields more binding energy than the one with a stronger tensor component (C). This is a general feature of BHF calculations for closed shell nuclei, employing phase-shift equivalent

potentials[15]), which obviously is valid also for binding energies obtained in shell-model calculations for open shell nuclei. (ii) The modification of the Dirac spinors in the medium contained in G_m reduces the calculated binding energy. This is also a feature already present in DBHF calculations and which can be understood as a reduction of the attractive components due the exchange of a scalar meson (σ). (iii) A smaller calculated binding energy is accompanied by a larger value of the oscillator parameter b for which the minimum is obtained. In the case of ^{6}Li and ^{7}Li one observes that the minimum value for G^A occurs for $b = 1.8\ fm$ although an almost equal value is obtained for $b = 1.6\ fm$. Thus a proper variational calculation using G^A interaction most certainly will find the minimum between the above two values of the oscillator parameter. A different behavior is observed with the other three interactions where, as the results of table 1 indicate, the minima are shifted to larger oscillator values. This is particularly evident in the case of the G_m^C results. This behavior is similar to features of DBHF calculations for ^{16}O, in which one finds that a larger tensor force and the inclusion of Dirac effects increase the calculated radii.

Table 1

Dependence of the binding energies of the Li isotopes on the oscillator parameter b

$b(fm)$	1.6	1.8	2.0	2.1
		^{6}Li		
G^A	-20.54	-20.83	-19.49	
G^C	-14.46	-15.85	-15.43	
G_m^A	-15.04	-16.64	-16.49	-15.93
G_m^C	-8.79	-11.48	-12.17	-12.00
		^{7}Li		
G^A	-26.47	-26.59	-24.63	
G^C	-18.89	-20.51	-19.75	
G_m^A	-19.54	-21.56	-21.24	-20.45
G_m^C	-11.77	-15.26	-16.03	-15.74
		^{11}Li		
G_m^A			-22.03	-21.68
G_m^C			-13.87	-14.32

Considering the results of table 1 as those of a restricted variational calculation we obtain a natural selection for the oscillator parameter to be considered in the rest of the calculation. Thus for investigations on ^{6}Li and ^{7}Li employing G^A, G^C or G_m^A interactions we adopt $b = 1.8\ fm$, while for the G_m^C interaction we consider

$b = 2.0\ fm$. The corresponding values for ^{11}Li are $b = 2.0\ fm$ and $b = 2.1\ fm$ for G^A_m and G^C_m interactions, respectively.

Fig. 1 shows the experimental and theoretical spectra of the low-lying positive parity states of ^{6}Li. The theoretical predictions on the electromagnetic properties of this nucleus, determined for all interactions discussed above, are compared to the experimental data[17]) in table 2.

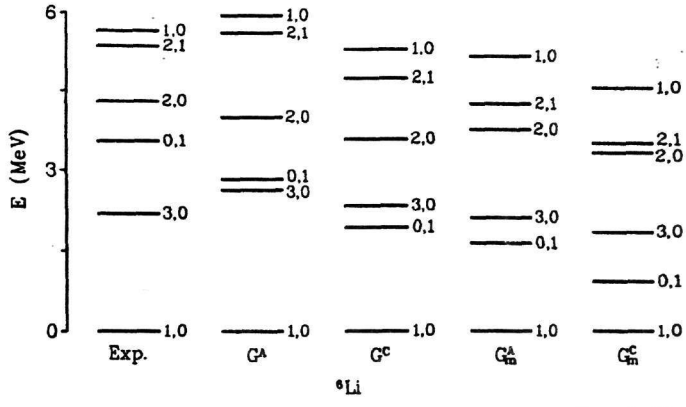

Figure 1: Low-lying spectra of ^{6}Li calculated with various G-matrices in the space of $(0+2)\hbar\omega$ excitations. All states have positive parity. Each level is labelled by J, T. The experimental information is from Ref. [17]).

Table 2

Electromagnetic properties of ^{6}Li determined with various G-matrices

Quantity	Units	Experiment	G^A	G^C	G^A_m	G^C_m
r_{ms}	fm	2.09 ± 0.02	2.34	2.39	2.40	2.64
μ	μ_ν	0.8220	0.8530	0.8453	0.8540	0.8524
Q_s	efm^2	-0.083	-0.302	-0.407	-0.099	-0.365
$B(E2; 3,0 \rightarrow 1,0)$	WU	16.5 ± 1.3	4.96	5.49	5.57	8.35
$B(M1; 0,1 \rightarrow 1,0)$	WU	8.62 ± 0.18	8.64	8.52	8.84	8.72
$B(E2; 2,0 \rightarrow 1,0)$	WU	6.8 ± 3.5	4.06	4.24	5.26	7.04
$B(M1; 2,1 \rightarrow 1,0)$	WU$\times 10^{-2}$	8.35 ± 1.5	0.04	0.09	2.2	0.06

As may be seen in fig. 1, the excitation energies of the ^{6}Li states with isospin $T = 0$ are rather insensitive on the interaction used and show a good agreement with the experimental data, whereas the position of the states with isospin $T = 1$ relative to the $T = 0$ states changes quite drastically with the choice of the interaction. This

behavior is particularly evident in the case of the $J = 0$, $T = 1$ state where one obtains excitation energies which differ by almost 2 MeV. The excitation energy of this state is underestimated using G^A and the agreement with the experiment becomes worse using G^C, G^A_m and G^C_m.

The four interactions produce quite similar results for most of the electromagnetic observables displayed in table 2. These results are also in reasonable agreement with the experimental data, bearing in mind that in our calculation we consider bare electromagnetic operators. One, however, observes that the G^C_m calculation predicts r_{ms} and $B(E2)$ values which are considerably larger than those obtained with the other interactions. This behavior can only partly be attributed to the larger value of the oscillator parameters b used in the G^C_m calculation. Therefore we conclude that the increase in the calculated radii as we go from interaction G^A to G^C_m describes the effect already observed in DBHF calculations for closed shell nuclei (see discussion above).

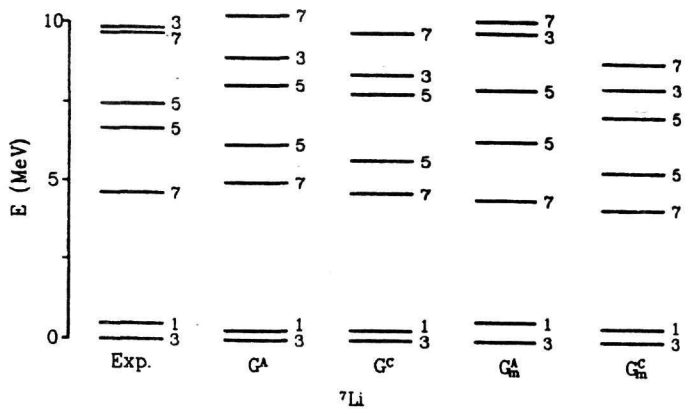

Figure 2: Low-lying spectra of ^{7}Li calculated with various G-matrices (see text) in the space of $(0+2)\hbar\omega$ excitations. All states have negative parity and $T = 1/2$. Each level is labelled by $2J$. The experimental information is from Ref. [17]).

Fig. 2 shows the experimental and theoretical spectra of the low-lying negative parity states of ^{7}Li. Unlike the case of ^{6}Li, discussed above, the four interactions considered in the calculation produce spectra which are quite similar to each other and also with the experimental one. It seems that the differences observed in the $T = 1$ spectrum as compared to the $T = 0$ states of ^{6}Li are getting less important for systems with more valence nucleons. In particular, the spectra obtained with the G-matrices derived from potential A , independent of the choice of the parameter m^*, are in close agreement with the data.

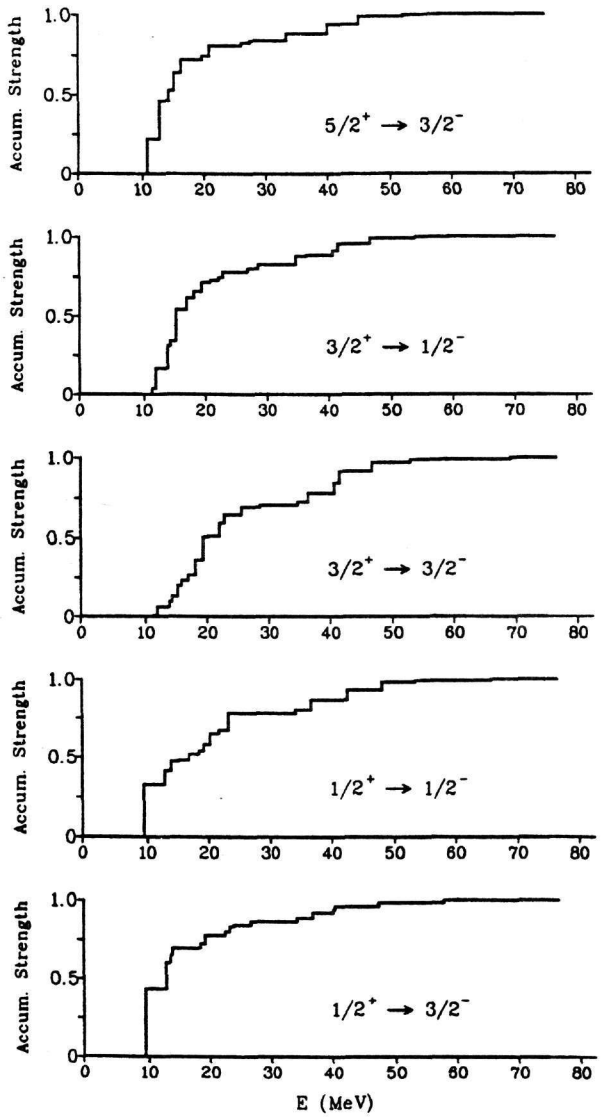

Figure 3: Distribution of the $E1$ strength among the $T = 1/2$ positive parity states of ^{7}Li. Only transitions leading to the ground state $3/2^-$ and to the first excited $1/2^-$ state are shown. The accumulated strength is normalized to 1 for the complete strength in each channel.

To calculate the dipole polarizability for ^{7}Li one needs to calculate the unnatural parity states which are connected by the $E1$ operator to both the ground and first excited states of this nucleus. These states have spins $1/2^+$, $3/2^+$ and $5/2^+$ while their isospin can be either $1/2$ or $3/2$. As discussed in sect. 2.2, these states are determined in the space of $(1+3)\hbar\omega$ excitations using the BAGEL approach. This approach selectively determines the states which have strong $E1$ coupling to the ground and first excited states. The results of this calculation are shown in fig. 3, which shows the energy position as well as the $E1$ strength for the $T = 1/2$ unnatural parity states. The results shown in fig. 3 correspond to the G^C_m interaction. As discussed below, for this interaction one obtains the largest, in magnitude, values of the τ_{ij} tensors.

As fig. 3 shows, the $E1$ strength is distributed over a large number of states in the energy range of 10 to about 70 MeV. One may also observe a spin dependence in the distribution. For example, in the case of the $1/2^+$ states about 40% of the strength is concentrated in the lowest state at about 9.5 MeV, while in the case of the $3/2^+$ states the strength is distributed over many states and one has to extend to about 25 MeV to exhaust 50% of the total strength.

In table 3 we list the theoretical predictions on the electromagnetic properties of ^{7}Li for all interactions considered in the calculation. Table 3 also includes the predictions of the calculation on the polarizability terms P, τ_{11} and τ_{12}. One should remark at this point that with the existing data on ^{7}Li it is not possible to obtain an estimate for P [6]) and thus the theoretical predictions for this quantity cannot be yet be compared with experiment.

Table 3

Electromagnetic properties of ^{7}Li determined with various G-matrices

Quantity	Units	Experiment	G^A	G^C	G^A_m	G^C_m
r_{ms}	fm	2.23 ± 0.02	2.41	2.45	2.46	2.71
μ	μ_ν	3.2564	3.0789	3.0918	3.1270	3.1339
$B(M1; 1/2 \rightarrow 3/2)$	WU	2.75 ± 0.14	2.39	2.36	2.39	2.38
$B(E2; 1/2 \rightarrow 3/2)$	WU	19.7 ± 1.2	7.72	8.74	9.25	13.7
$B(E2; 7/2 \rightarrow 3/2)$	WU	4.3	3.69	4.01	5.65	6.15
Q_s	efm^2	-4.00 ± 0.06	-2.54	-2.70	-2.81	-3.39
$B(E2; 3/2 \rightarrow 1/2)\uparrow$	e^2fm^4	7.27 ± 0.12	3.14	3.55	3.76	5.56
P	fm^3		0.095	0.109	0.110	0.164
τ_{11}	fm^3	-0.12 ± 0.07	-0.050	-0.056	-0.057	-0.084
τ_{12}	fm^3	-0.148 ± 0.012	-0.049	-0.055	-0.053	-0.080

As may be seen in table 3, the four calculations produce very similar values for the magnetic moment of the ground state as well as for the $B(M1)$ corresponding

to the deexcitation of the first excited state. On the other hand, one observes a dependence of the r_{ms}, the $E2$ matrix elements and the dipole polarizability terms on the interaction employed. This behavior is more pronounced in the G_m^C results, but one should remember that these were obtained with a larger b value. Generally, the G_m^C results are in closer agreement with experiment than those obtained with the other three interactions.

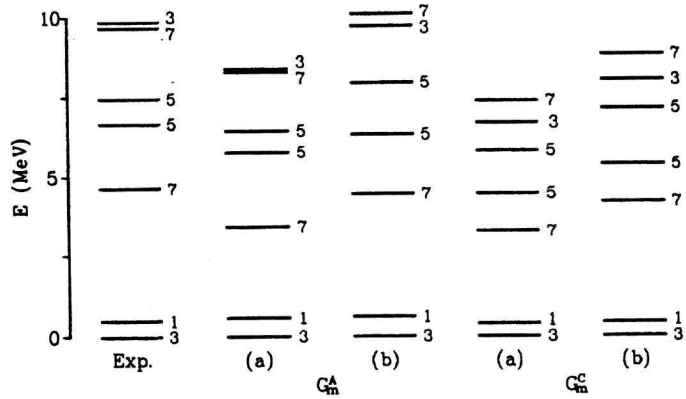

Figure 4: Low-lying spectra of ^{7}Li calculated with interactions G_m^A and G_m^C (see text). The spectra labelled (a) have been determined in the $0\hbar\omega$ space, while those labelled (b) in the $(0+2)\hbar\omega$ space. All states have negative parity and $T = 1/2$. Each level is labelled by $2J$.

Table 4

Effects of configuration space on the electromagnetic properties of the low-lying states of ^{7}Li

Quantity	Units	Experiment	G_m^A		G_m^C	
			$0\hbar\omega$	$(0+2)\hbar\omega$	$0\hbar\omega$	$(0+2)\hbar\omega$
B.E	MeV	39.25	14.11	21.24	9.59	16.03
r_{ms}	fm	2.23 ± 0.02	2.50	2.46	2.78	2.71
μ	μ_ν	3.2564	3.1431	3.1270	3.1339	3.1375
$B(M1; 1/2 \rightarrow 3/2)$	WU	2.75 ± 0.14	2.45	2.39	2.45	2.38
$B(E2; 1/2 \rightarrow 3/2)$	WU	19.7 ± 1.2	4.17	9.25	6.67	13.7
$B(E2; 7/2 \rightarrow 3/2)$	WU	4.3	1.64	4.06	2.61	6.15
Q_s	efm^2	-4.00 ± 0.06	-2.00	-2.81	-2.46	-3.39
$B(E2; 3/2 \rightarrow 1/2)\uparrow$	e^2fm^4	7.27 ± 0.12	1.70	3.76	2.71	5.56

We conclude our study of ^{7}Li by examining the effects of configuration space on the properties of this nucleus. To study these effects we made additional calculations

in the space of $0\hbar\omega$ configurations for the natural parity states and $1\hbar\omega$ for the unnatural parity ones. In fig. 4 we compare the low-lying energy spectrum obtained in the restricted space with that of the extended space while table 4 lists the remaining properties of the natural parity states. As the results shown in both fig. 4 and table 4 indicate, there is a drastic improvement in the theoretical predictions when one extends the model space.

The polarizability quantities τ_{12}, τ_{11} and P have also been calculated for different choices of model spaces and the results are shown in table 5. In one calculation, termed "small" in the table, the natural parity states have been calculated in the $0\hbar\omega$ space and the unnatural in the $1\hbar\omega$ space. In another calculation, termed "medium" in table 5, the space of the natural space is extended to $(0+2)\hbar\omega$ excitations, while the unnatural parity states are again determined in the $1\hbar\omega$ space. Finally, "large" in table 5 denotes the results obtained in the complete space used in this calculation.

Table 5

Effects of configuration space on the dipole polarizability of ^{7}Li

Space	τ_{12} (fm^3)	τ_{11} (fm^3)	P (fm^3)
Small	-0.0431	-0.0463	0.197
Medium	-0.0409	-0.0432	0.095
Large	-0.0801	-0.0838	0.164
Experiment	-0.148	-0.12	

As may be seen in table 5, the monopole polarizability P obtains its maximum value in the small space. On the other hand, the values obtained in this space for the two quadrupole tensors are about 50% in magnitude of those obtained in the complete space. The smallest values in magnitude are obtained for all three quantities in the medium space calculation. The reason for this behavior is twofold: i) the coupling between $2\hbar\omega$ and $1\hbar\omega$ configurations is weak and ii) there is a considerable increase in the energy denominators in eqs (5) and (7) as can be deduced from the increase of binding energies listed in table 4.

The results in both tables 4 and 5 clearly suggest the importance of high-lying configurations which affect both the properties of the low-lying states, as well as the polarizability effects. Extrapolating this behavior one expects a further improvement in the shell-model results if even higher configurations, like $4\hbar\omega$ for the natural parity states and $5\hbar\omega$ for the unnatural parity ones could be included. Such an enlargement of the model space could most probably make the predictions of the shell-model similar to those of the cluster model.

The nucleus ^{11}Li is known[8]) to be a loosely bound system with a very small two-neutron separation energy. Therefore, the need for considering a very large shell-model space would be more pronounced for this nucleus than for ^{7}Li. Hence, we do not

expect our parameter free calculation to account for all the properties of ^{11}Li despite the fact that we employ a space in which all configurations up to $3\hbar\omega$ excitation are included.

From the available experimental data on ^{11}Li, one knows that this nucleus has a very large r_{ms} value of 3.16 ± 0.11 fm [10]) and in addition there is evidence that the first excited state at 1.2 MeV has positive parity[18]). From the ^{7}Li investigation, described above, we know that such effects are best described in our model if one uses the G_m^A and G_m^C interactions. Therefore, the results to be discussed below were obtained with the use of these two interactions.

Fig. 5 shows the predictions of our calculation on the low-energy spectrum of ^{11}Li. As this figure shows the calculation predicts that the first excited state of ^{11}Li is a $1/2-$ state followed by a series of positive parity states the lowest of which, a $3/2+$, appears at about 4 MeV. As discussed above, one expects that the results shown in fig. 5 could change considerably by the inclusion of higher configurations in the model space.

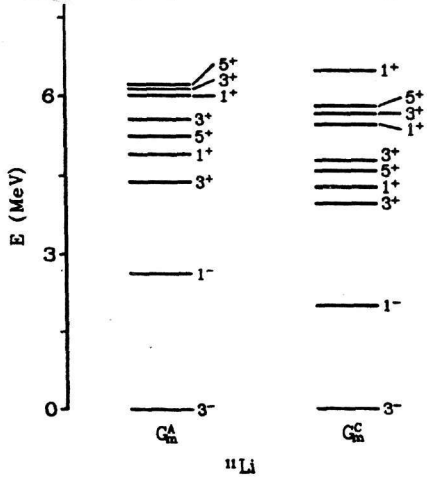

Figure 5: Low-lying spectra of ^{11}Li calculated with interactions G_m^A and G_m^C (see text). All states have $T = 5/2$. Each level is labelled by $2J^\pi$.

Fig. 6 shows the energy position and the distribution of $E1$ transition strengths to the ground state for the $T = 5/2$ positive parity states of ^{11}Li. The results shown in fig. 6 have been obtained using the G_m^C interaction which, as evidenced from fig. 5, produces lower excitation energies for the unnatural parity states. A comparison of the distributions shown in figs. 3 and 6 shows a significant difference between ^{7}Li and ^{11}Li. In the latter, particularly in the $3/2^+$ case, one observes a low-energy component in the distribution. Specifically, the lowest $3/2^+$ state, predicted to be at 3.86 MeV, carries about 4% of the total $E1$ strength. This feature could be interpreted to correspond to the *soft dipole mode* speculated for this nucleus[8-9]).

Table 6
Properties of ^{11}Li

Quantity	Exper.	G_m^A	G_m^C
r_{ms} (fm)	3.16 ± 0.11	2.81	2.97
μ (μ_ν)	3.6673 ± 0.0025	3.6908	3.6890
Q_s (efm^2)	-3.12 ± 0.45	-3.48	-3.92
τ_{11} (fm^3)		-0.0149	-0.0624
P (fm^3)		0.238	0.375

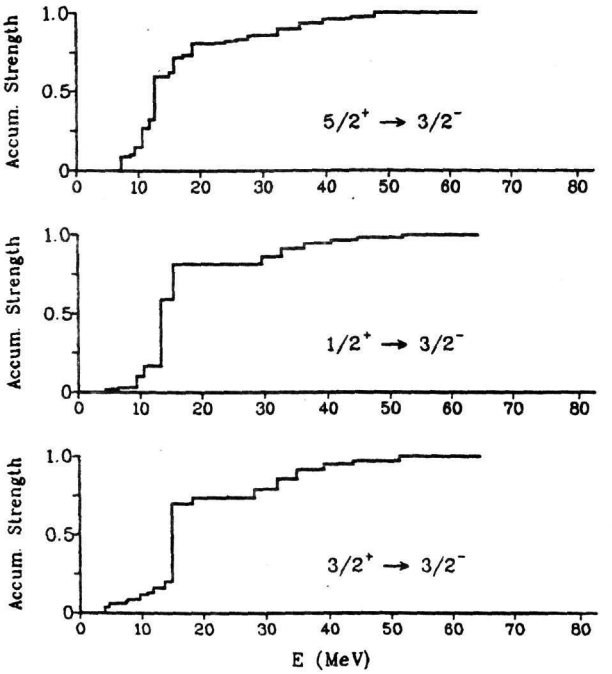

Figure 6: Distribution of the $E1$ strength among the $T = 5/2$ positive parity states of ^{11}Li. Only transitions leading to the ground state are shown.

Finally, in table 6 we summarize the predictions of our calculation regarding the ground state properties of ^{11}Li. As this table shows the calculation accounts satisfactorily for the r_{ms} and the magnetic and quadrupole moments of this nucleus. This is particularly true for the r_{ms} value obtained with the G_m^C interaction. It is interesting also to note in table 6 that the calculation predicts quite larger P values than those obtained for ^{7}Li with the same interactions. This should be attributed to a) that a

larger b value is used in the ^{11}Li calculation and b) that the excitation energy of the positive parity states is greatly reduced. On the other hand the ^{11}Li calculations predict smaller τ_{11} values than those obtained for ^{7}Li. This behavior should be attributed to the strong cancellation among the contributions of the various J,T positive parity states. It would be of considerable interest if values of P and τ_{11} were obtained in future experiments on ^{11}Li, since these will provide a useful test of our calculation.

Conclusions

Results of shell-model calculations for the isotopes ^{6}Li, ^{7}Li and ^{1}1Li are presented, which consider configurations within various major shells. Realistic hamiltonians are considered, which contain the kinetic energy and a NN interaction derived from modern OBE potentials[14]). The effects of NN short-range correlations are taken into account by solving the Bethe-Goldstone equation for these potentials, considering a Pauli operator which is consistent with the shell-model configurations taken into account. No further renormalization of the hamiltonian and the operators for the electromagnetic transitions has been made since it is the aim to account for those long-range correlations by a sufficiently large shell-model space. The main conclusions can be summarized as follows:

- The bulk properties (binding energies, radii) calculated for the open shell nuclei show a similar dependence on the OBE interaction used as it has been observed in DBHF calculations for closed shell nuclei: NN interactions with a stronger tensor component yield less binding energy as a phase-shift equivalent potential with a weaker tensor force; the modification of the Dirac spinors for the nucleons in the medium reduces the calculated binding energy; a smaller binding energy is correlated with a larger value for the radius.

- The calculated excitation spectra are weakly depending on the NN interaction. Only in the case of ^{6}Li a strong dependence of the energies for the states with isospin $T = 1$ relative to those with $T = 0$ is observed. A good agreement with the experimental data is achieved if a large model space is considered.

- Also the calculated electromagnetic properties show a good agreement with the empirical data, keeping in mind that the present calculation does not contain any adjustable parameter.

- The results of the present investigation clearly indicate that the polarizability tensors τ_{11} and τ_{12} for ^{7}Li depend strongly on the model space. Thus it appears that to improve further the agreement with the experimental data one needs to go beyond those model spaces considered in the present approach. Such an expansion of the model space is currently very difficult to attempt due to the exceedingly large number of shell-model configurations involved.

References

[1] K. Alder and A. Winther, Electromagnetic Excitation (North Holland, Amsterdam, 1975)

[2] J. de Boer and A. Winther, Coulomb Excitation, ed K. Alder and A. Winther (Academic Press, New York, 1966)

[3] A. Weller, P. Engelhof, R. Čaplar, O. Karban, D. Krämmer, K.H.- Möbious, Z. Moroz, K. Rusek, E. Steffens, G. Tungate, I. Koenig and D. Fick, Phys. Rev. Lett. **55** (1985) 480

[4] W.J. Vermeer, R.H. Spear and F.C Barker, Nucl. Phys. **A500** (1989) 212

[5] F.C. Barker, Y. Kondō and R. Spear, Aust. J. Phys. **42** (1989) 597

[6] H.-G. Voelk and D. Fick, Nucl. Phys. **A530** (1991) 475

[7] T. Kobayashi, S. Shimoura, I. Tanihata, K. Katori, K. Matsuta, T. Minamisoto, K. Sugimoto, W. Müller, D.L. Olson, T.J.M. Symons and H. Wieman, Phys. Lett. **232B** (1989) 51

[8] P.G. Hansen and B. Jonson, Europhys. Lett. **4** (1987) 409

[9] Y. Suzuki, K. Ikeda and H. Sato, Prog. Theor. Phys. **83** (1990) 180

[10] F. Ajzenberg-Selove, Nucl. Phys. **A506** (1990) 1

[11] J.P. Elliott and T.H.R Skyrme, Proc. Roy. Soc. **A232** (1953) 561

[12] L.D. Skouras and H. Müther, Nucl. Phys. **A515** (1990) 93

[13] H. Müther and P.U. Sauer, *Computational Methods in Nuclear Physics* **II**, (Springer 1992) to be published

[14] R. Machleidt, Adv. in Nucl. Phys. **19** (1989) 189

[15] H. Müther, R. Machleidt and R. Brockmann, Phys. Rev. **C42** (1990) 1981

[16] A.H. Wapstra and G. Audi, Nucl. Phys. **A432** (1985) 1

[17] F. Ajzenberg-Selove, Nucl. Phys. **A490** (1988) 1

[18] H.T. Fortune, private communication.